Available online at www.sciencedirect.com
SCIENCE DIRECT
Sensors and Actuators A 128 (2006) 109–115
SENSORS AND ACTUATORS A PHYSICAL
www.elsevier.com/locate/sna

Stiction problems in releasing of 3D microstructures and its solution

Dongmin Wu, Nicholas Fang, Cheng Sun, Xiang Zhang *

5130 Etcheverry Hall, NSF Nano-scale Science and Engineering Center, University of California Berkeley, CA 94720-1740, United States

Received 8 September 2005; received in revised form 11 December 2005; accepted 17 December 2005
Available online 23 January 2006

Abstract

Micro-stereolithography (μSL) is capable of fabrication of highly complex three-dimensional (3D) microstructures by selectively photo-induced polymerization from the monomer resin. However, during the evaporative drying of structures from liquid resin, the 3D microstructures often collapse due to the capillary force. In this work, a theoretical model is developed to analyze the deflection and adhesion between thin polymer beams under capillary force. The detachment length of the test structures and adhesion energy of a typical μSL polymer (HDDA) are obtained experimentally which are important for MEMS structure design. Finally, we successfully developed a sublimation process to release the 3D microstructures without the adhesion.

Keywords: Micro-stereolithography; Photopolymerization; Surface tension; MEMS

1. Introduction

With the capability of building structures in an additive, layer-by-layer process at micrometer scale, micro-stereolithography (μSL) enables the fabrication of highly complex, three-dimensional microstructures, which is critical to the development of advanced microelectro-mechanical systems (MEMS) devices [1]. Although relatively simple 3D microstructures can be fabricated by silicon micromachining, it remains still a challenge to fabricate truly complex 3D microstructures, because of the limited layers one can use in silicon micromachining. Inspired by the rapid prototype technique, Ikuta first introduced the stereolithography technique into microscale fabrication [2]. There are several distinct advantages making this method a unique and promising technique for 3D microfabrication. First, micro-stereolithography is an additive process. In μSL, polymeric structures are fabricated out of UV curable liquid resin upon photo-induced polymerization reactions. The final 3D structure is formed by adding the polymers layer-by-layer. Compare with etching or other removal process, additive process is more convenient for 3D fabrication of complex structures. Second, it requires no physical masks. Third, μSL can fabricated very high-aspect-ratio structures without limitations in vertical direction. In the silicon micromachining, due to the alignment requirement, number of layers of the structure is limited. Fourth, μSL is highly compatible with the computer aided design (CAD) making it an agile fabrication method. Using the auto slicing technique and computer controlled scanning stages, 3D structures can be copied directly from the computer model into the real polymer structures in a short time. Continuous efforts have been made to optimize the μSL. Using large NA lens, local polymerization with resolution smaller than 1 μm have been achieved [3]. Two-photon polymerization has been explored to increase the resolution of μSL process [4]. Although the working material of μSL is polymer, other materials can also been applied. Metal structures can be fabricated by using the polymer structure as mold for casting or electroplating. Ceramic structures can be achieved directly by mixing the green powder with the liquid resin [1,5].

After photofabrication, un-polymerized resin has to be rinsed out to obtain the free standing 3D structures. Strong capillary force will develop during the final evaporative drying which deform the microstructures and cause the adhesion and collapse of polymer structures. The phenomena have been referred to as "stiction", a problem that has been studied previously in silicon surface micromachining [6–11].

The interfacial attractive forces involved in the stiction phenomena can be attributed to Van de Waals force, electrostatic force, and hydrogen bonding. People use the term of interfacial adhesion energy γ_s to describe the strength of the attrac-

* Corresponding author.
E-mail address: xiang@berkeley.edu (X. Zhang).

0924-4247/$ – see front matter © 2006 Elsevier B.V. All rights reserved.
doi:10.1016/j.sna.2005.12.041

tive force. Typically, the adhesion energy is in the range of 500–2000 mJ/m^2 for crystalline solids and 5–100 mJ/m^2 for polymers [6]. If the adhesion energy is not strong enough to withstand the restoring elastic force, the deformed structures will bounce back to original shape. The competition of the restoring elastic force and adhesion energy defines a critical length (detachment length), below which the structures will be able to return back to the un-deformed state. Determination of the detachment length and applying it in the design of the microstructures is essential to enhance the process reliability of μSL. We have reported a simple method to measure the adhesion force between the polymer structures in Ref. [12]. In this paper, we will discuss the method more detailed and develop a new releasing technique for μSL fabricated structures to reduce the stiction problem.

2. Background/theory

As we discussed before, μSL allows direct fabrication of polymeric structures from computer generated 3D solid model in a layer-by-layer additive manner. A typical μSL system is shown in Fig. 1. The UV beam from the light source is directed to the beam shaping component, which controls the pattern shape at the image plane. The 3D computer model is sliced into a series of 2D layers with specified thickness. Then, the 2D image of each slide is transferred to the beam shaping component in sequence to expose the UV curable resin resulting a thin polymer layers which can be stacked layer-by-layer to form a 3D structure. After one polymer layer is solidified, the translation stage moves downward, and allows a new liquid layer to be formed on top and process repeats. The UV resin is a mixture of monomer and photo-initiator. When illuminated by UV light, the photo-initiator will decomposed and generate radicals which initiates the polymerization. Because of the absorption in UV resin, the light intensity will decrease when propagating away from the surface and the polymerization always starts from the interface

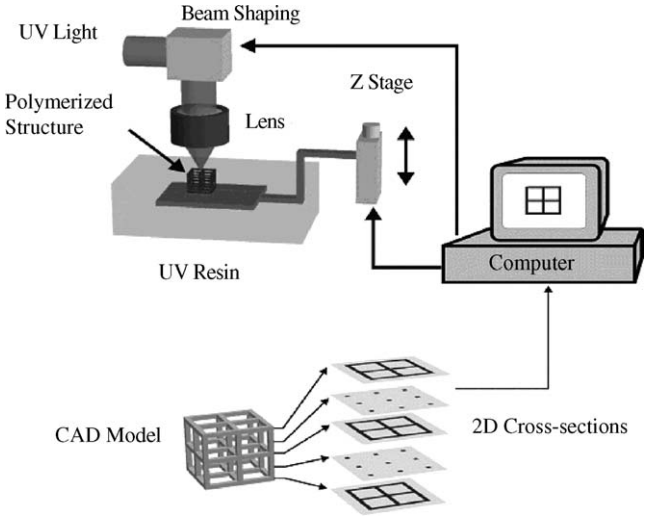

Fig. 1. The set up of μSL system. The computer slices the CAD model into a series of 2D cross-sections and transfers the 2D image to the beam shaping element to control the local exposure of each layer.

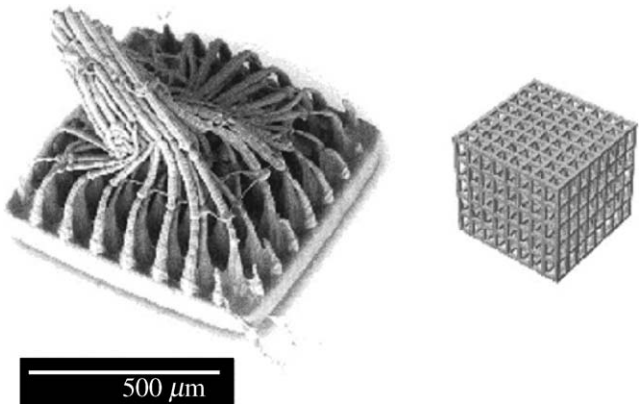

Fig. 2. A collapsed 3D microstructure fabricated by μSL. The polymer beams are bend under the capillary force during evaporation, and adhered together after drying. Right inset is the original 3D solid model.

and stops at certain distance from the surface (curing depth) for a given light intensity and exposure time. The relationship between the curing depth (D), light intensity (I), and exposure time (t) is described by following equation:

$$D = D_p \ln\left(\frac{It}{E_c}\right) \quad (1)$$

where D_p is the penetration depth of UV light in the resin and E_c is the critical dose. For a given UV resin, D_p and E_c are constants. Eq. (1) is defined as the working curve of the resin.

In macro-scale stereolithography, evaporation drying is sufficient to release the fabricated 3D polymer structures because volume force is stronger than surface tension at macro-scale [13]. However, in μSL, as discussed above, the strong capillary force will cause stiction problem during evaporation drying. Fig. 2 shows a collapsed μSL fabricated microstructure due to the capillary force during the evaporative releasing. The original designed structure is a 3D cubic lattice.

The adhesion of silicon beams to substrate, known as "stiction" problem, has been found and studied in the 2D silicon surface micromachining [6,7]. It has been referred as a major factor influences the reliability of the silicon surface micromachining. In μSL, the adhesion among different parts of the 3D microstructures is more prominent and may also leads the total structure failure, as shown in Fig. 2. Due to the complexity of the geometry, stiction problems in 3D microfabrication are more likely to occur within the microstructure and it is different than the case for 2D microfabrication, which only concern the stiction from microstructure to the substrate. Thus, the model established in Mastrangelo's work [6,7] need to modified to study the stiction problem specific for the 3D microfabrication. To simplify the problem and isolate the influence of substrate, we designed a test structure with two parallel beams on top of high-aspect-ratio supporting posts (Fig. 3). The parameters obtained from this test structure, e.g. the surface adhesion energy of photopolymer, are not geometry specific and thus, will be used to design the 3D microstructure to avoid stiction problem. Fig. 3(b) illustrates the mechanism of stiction during evaporation drying. The beams are distorted by capillary force from the captured liquid between them, and are kept adhering to each other by interfacial

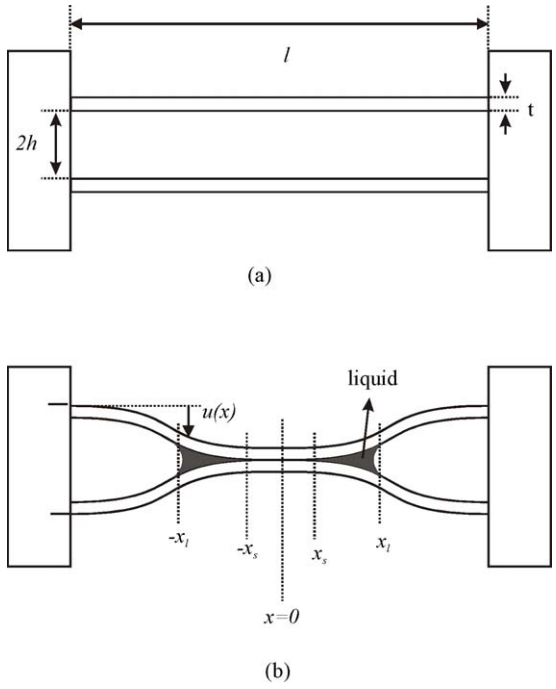

Fig. 3. Schematic of the model used to calculate the detachment length l_d in μSL. (a) Top view of the designed beams; (b) the beams are distorted during evaporation drying by the capillary force, the shaded regions represent the solvent liquid captured between the beams.

adhesion force. $2x_s$ is the length (adhesion length) of the part where two beams adhere together, l and t are the original length and width of beams, respectively, and $2h$ is the spacing between parallel beams.

We consider the energy stored in the system shown in Fig. 3(b) to derive the detachment length. The total energy of the system comes from three major sources: the elastic energy U_e of the deformed polymer beams, the solid–liquid surface energy U_{sl} stored in the wetted areas, and the solid–solid surface energy U_{sc} stored in the contact areas. Since the two beams under consideration are identical, we only have to solve the stored energy for one beam. From Euler's approximation, the elastic energy of one beam under deflection can be written as

$$U_e = \frac{EI}{2}\int_{-l/2}^{l/2}\left(\frac{d^2u}{dx^2}\right)^2 dx \tag{2}$$

where E is the Young's modulus of polymer, I the moment of inertia of the beam, and $u(x)$ is the position of the deflected beam. The solid–liquid surface energy and solid–solid surface energy is given by

$$U_{sl} = -4\gamma_l w\cos\theta_c(x_l - x_s) \tag{3}$$

and

$$U_{sc} = -2\gamma_s w x_s \tag{4}$$

where w is the thickness of the beam, θ_c the contact angle, and γ_l and γ_s are the surface energy of liquid and solid, respectively. Thus, the total energy of the system is

$$U_t = U_e + U_{sl} + U_{sc} \tag{5}$$

The displacement of the beam $u(x)$ can be expressed as [6]:

$$u(x) = h\left[1 - \left(\frac{x - x_s}{l/2 - x_s}\right)^2\right] \tag{6}$$

When the beam is at equilibrium, x_s and x_l does not change, e.g.

$$\frac{\partial U_t}{\partial x_l} = \frac{\partial U_t}{\partial x_s} = 0 \tag{7}$$

From the equations above, and let $x_l = x_s$, which means the liquid is totally evaporated, we derive the adhesion length, $2x_s$, of the drying beams:

$$2x_s = l\left[1 - \left(\frac{128}{5}\frac{Eh^2t^3}{\gamma_s l^4}\right)^{1/4}\right] \tag{8}$$

The detachment length is defined as

$$l_d = \left(\frac{128E}{5\gamma_s}\right)^{1/4}(h^2t^3)^{1/4} \tag{9}$$

As mentioned before, the detachment length is a critical parameter. When the designed beam length exceeds the detachment length, stiction will most likely occur. We will discuss how to obtain the detachment length experimentally in the next section. It is also possible to derive the polymer–polymer surface adhesion energy γ_s from Eq. (9) given the detachment length and the Young's modulus. Based on this model, we can provide a relatively simple, indirect method to measure the γ_s.

3. Characterization of stiction

The test structures are fabricated by a projection μSL system developed in our lab [14]. The UV curable resin contains 1,6-hexanediol diacrylate (HDDA) monomer and 5 wt.% benzoin ethyl ether as photo-initiator. A mercury arc lamp is used as UV light source. To select the i line (365 nm) emission of the mercury lamp, a narrow band filter (10 nm bandwidth) is put inside the optical path. The optimized exposure dose in ambient environment is 200 mJ/cm^2, correspond to a curing depth of 5 μm. After fabricated, the polymer structures are rinsed in isopropanol alcohol (IPA) and then dried through evaporation in air.

The dried structures were observed using environmental scanning electron microscope (N-SEM), which does not require the samples being conductive. Fig. 4(a) is the N-SEM image of two pairs of beams released by evaporation method. The picture clearly shows that the beams stick each other at the center, which agrees with our model. The beams in Fig. 4(b) is released by sublimation method, which we will discuses later. On the other hand, because we purposely designed the beam far away from the substrate, no adhesion was observed between beam and substrate. The two test structures have same beams length, but different width. The adhesion lengths can be measured directly from N-SEM pictures. To study the dependence of adhesion length on the width and spacing, we fabricated a group of test structures with same length and spacing, but different

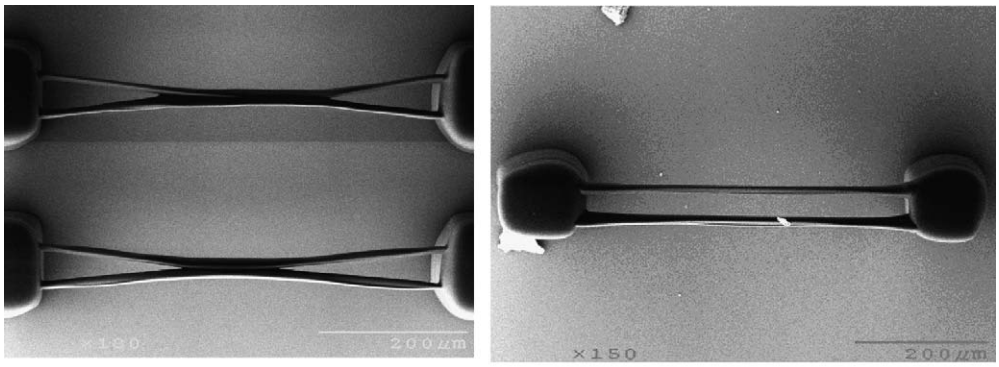

Fig. 4. SEM picture of suspended beams (top view). The beam length is larger than the detachment length. (a) Released by evaporation; (b) released by sublimation. The scale bar is 200 μm.

width. After releasing these structures, we measured the adhesion lengths and beam width. Fig. 5 shows the experimental data of adhesion lengths as a function of $(h^2t^3)^{1/4}$. The curve was fitted linearly according to Eq. (8). At point $x_s = 0$, the value of $(h^2t^3)^{1/4}$ corresponded to the specific detachment length l_d (in this case, $l_d = 525$ μm, which is predetermined when it was fabricated) was found.

With the same approach, we derived the geometry factor $(h^2t^3)^{1/4}$ corresponding to different detachment lengths. To do this, we fabricated varies groups of beams with different lengths (from 300 to 600 μm). Each group of the beams has same length, which corresponding to one data point in Fig. 6. Within each group, we measured the adhesion length and used the method mentioned in last paragraph to determine the value of $(h^2t^3)^{1/4}$ for the detachment length. The data was plotted in Fig. 6, and fitted linearly as a function of $(h^2t^3)^{1/4}$. The slope of the fitting curve is $(5\gamma_s/128E)^{-1/4}$, from Eq. (9). While applying Young's modulus of HDDA (930 MPa) [15], we calculated the value of γ_s for HDDA is 72 mJ/m^2.

The linearity of the curve indicates good experimental agreement with the theory. Eq. (9) predicts that detachment length is

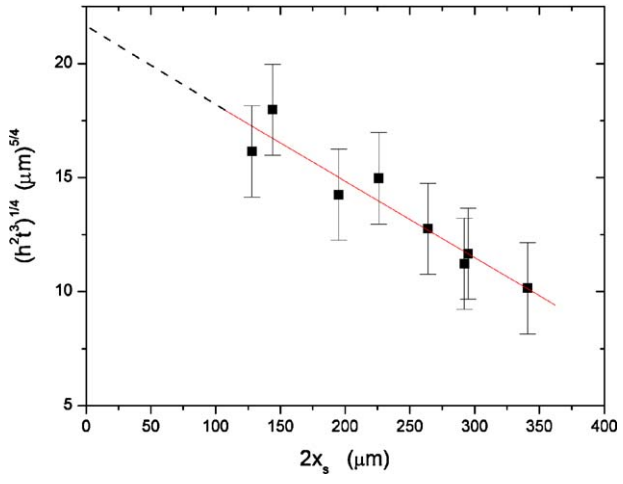

Fig. 5. Plot of the adhesion length. The beam length is fixed to 525 μm for each point. The linear fitting is according to Eq. (8). The geometry factor $(h^2t^3)^{1/4}$ corresponding to detachment is derived at the point where $2x_s$ equals to zero.

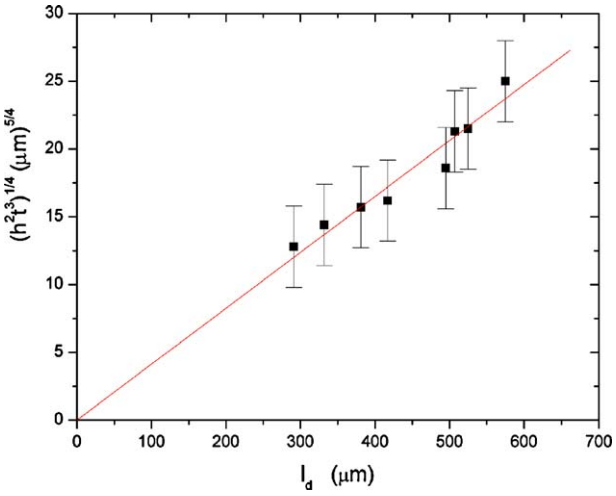

Fig. 6. Relationship between the detachment length l_d and $(h^2t^3)^{1/4}$. The value of $(h^2t^3)^{1/4}$ corresponding to each detachment length is derived by the method shown in Fig. 5. From the slop of the fitted line, we can calculate the surface energy of HDDA according to Eq. (9).

a weak function of polymer surface energy γ_s, since it is proportional to $\gamma_s^{-1/4}$. Therefore, modification of the polymer surface will not result in a significant increase of detachment length. On the other hand, l_d has a stronger dependence on scale (l_d is proportional to $(h^2t^3)^{1/4}$), which means decreasing the dimension D of polymer structures will decrease detachment length in a factor of $(D)^{5/4}$, if keeping the same shape. This explains why adhesion is significant in μSL when using evaporation drying. The detachment lengths and polymer surface energy γ_s we obtained from experiment can be used in the designing of polymer structures to reduce the stiction problem, and to increase the reliability of μSL fabrications.

4. Solution: sublimation drying

There are several methods to reduce the stiction problem. Choosing low surface tension liquid to rinse the microstructures is one of the options. This will decrease the capillary force developed during evaporation. If the surface tension induced capillary

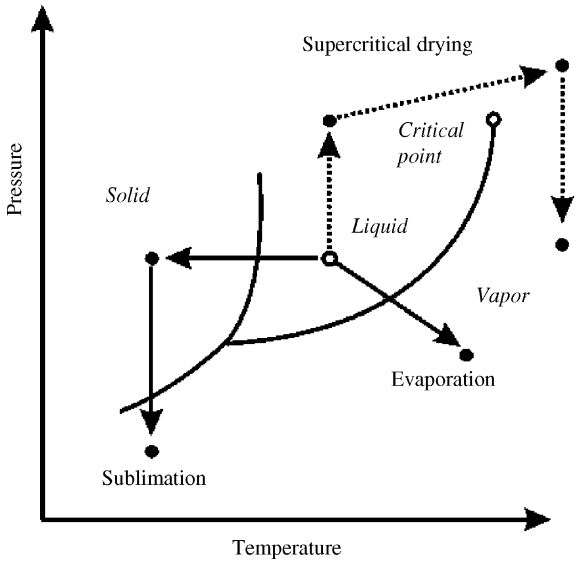

Fig. 7. Phase diagram of normal materials. We have three choices to release the microstructures from the liquid: evaporation, supercritical drying, and sublimation.

force is not strong enough to attract the microstructures contact each other or touch to the substrate, stiction will not occur. However, the effect of this method is limited because when the dimension scales down, capillary force will eventually increase and weights over volume force. The second method is modifying the surface property of polymer to decrease the surface energy γ_s [11]. It is not widely used because of the sophistication of chemical treatment. Also, as we mentioned before, detachment length is a weak function of polymer surface energy γ_s, which indicates that surface modification will not be an efficient way to reduce the stiction problem. To address this problem effectively, different releasing processes other than evaporation drying are needed to avoid the liquid–solid interface. There are two drying techniques available for this purpose: supercritical drying [9] and sublimation drying [8,10], both do not involve the liquid phase (Fig. 7). Therefore, no surface tension induced capillary force will develop during drying. We took the sublimation approach to address the stiction problem, because it is easy to access and can be optimized for μSL.

Among a variety of solvents that may be selected, we chose *t*-butyl-alcohol as the working medium, because its melting point is near the room temperature (Table 1). This enables us to eliminate the bulky refrigeration set up used in past. In addition, the relatively high vapor pressure of *t*-butyl-alcohol ensures a short sublimation time (less than 30 min). However, *t*-butyl-alcohol has its drawbacks: it will absorb water vapor from atmosphere and form droplet during sublimation drying. This will influence

Table 1
Material properties of some liquids

Material	Melting temperature (°C)	Boiling temperature (°C)	Vapor pressure
t-Butyl-alcohol	26	82.2	27 Torr at 20 °C
IPA	−88	82	33 Torr at 20 °C
Water	0	100	17.5 Torr at 20 °C

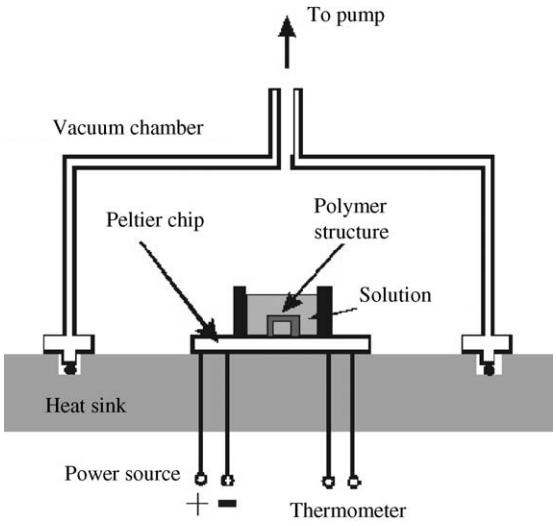

Fig. 8. The sublimation set up. The desiccator connected to the vacuum chamber is not shown in this figure.

the performance of the process. Therefore, special consideration must be paid for moisture control.

In our set up, the sample to be released is placed inside a small vacuum chamber (a bell jar) with a solid-state refrigerator. A desiccator is connected to the vacuum chamber in order to reduce the moisture level from the inlet. The solid-state refrigerator is made of a Peltier chip embedded in a thick metal plate. The Peltier chip is small and can be totally enclosed in a vacuum chamber of 4 in. diameter. With this advantage, solidifying and sublimation can be done without breaking the chamber sealing, which further reduces the absorption of moisture. The cooling speed is controlled by adjusting the current going through the Peltier chip. In addition, a pressure gauge and thermometer is used to monitor the working pressure and temperature, respectively.

A typical sublimation process starts from immersing the polymer structures in a small IPA bath for more than 5 min to remove the un-polymerized resin. It is followed by gradually replacing IPA by dispensing *t*-butyl-alcohol into the immersed sample and keeping the bath with constant volume of liquid solvent. After all solvent is replaced in the bath, the wet sample, together with the solution and container, is placed on top of Peltier chip (Fig. 8). Refrigeration will start after the chamber is sealed. To reduce stress development during crystallization of *t*-butyl-alcohol, the sample temperature is decreased slowly. When the liquid solvent is totally frozen, pumping will begin till all the *t*-butyl-alcohol solid in the container disappears.

To compare with evaporation drying, test beams in Fig. 4(b) are designed such that their lengths are longer than the detachment length we obtained from the experiment of evaporation drying. The test structure in Fig. 4(b) is then released using the sublimation method we discussed above. The result of sublimation drying shows no adhesion occurs. More examples of sublimation drying is shown in Fig. 9. The structure in Fig. 9(a) is an 800 μm cubic mesh similar to the structure shown in Fig. 2, but released using sublimation. Fig. 9(b) is a lattice of high-aspect-ratio (>30) polymer cylinders. Because the ends of the

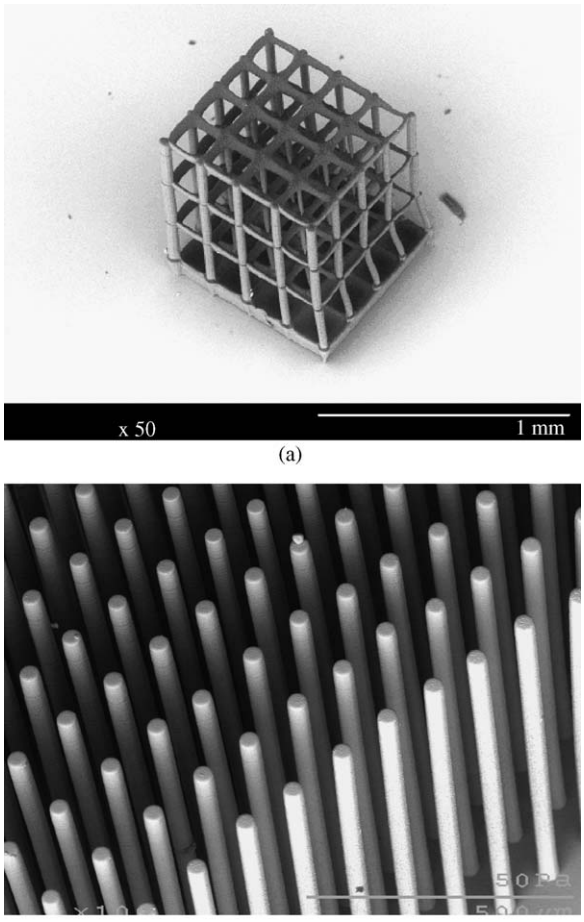

Fig. 9. Free standing 3D microstructures after sublimation drying. No adhesion between polymer beams observed. (a) A 800 μm cubic mesh with 200 μm spacing between beams; (b) a lattice of high-aspect-ratio polymer cylinders. The diameter of the cylinder is 30 μm, the height is 1000 μm. The scale bar in the picture is 500 μm.

cylinders are free, these wire-like structures are extremely vulnerable to the stiction problem.

The success of releasing benefits from the elimination of liquid–solid interface in sublimation drying. However, we also observed the structures crack sometimes after the releasing. This may be caused by the stress developed during the freezing of working medium. Decreasing the temperature slowly and smoothly will reduce the stress development and the probability of crack.

5. Summary

In this work, we studied the stiction problem of polymer structures fabricated by μSL. A series of test structures were fabricated and analyzed. We measured the adhesion length of parallel beams with different beam parameters and derived the detachment lengths. By fitting the curve of detachment length, the solid surface tension of HDDA was found to be 72 mJ/m^2. This work provides an indirect way to measure the solid surface tension of materials. A sublimation drying set up is used to replace evaporation drying as the releasing process for μSL. The results of sublimation experiment show no stiction problems even when beam lengths are longer than the detachment length in evaporation drying.

Acknowledgments

The authors wish to thank Professor C.J. Kim for the insightful discussion and Mr. Atif Noori for the help during setting up the sublimation instrument.

References

[1] X. Zhang, X.N. Jiang, C. Sun, Micro-stereolithography of polymeric and ceramic microstructures, Sens. Actuators A 77 (1999) 149–156.
[2] K. Ikuta, K. Hirowatari, Real three-dimensional microfabrication using stereolithography and metal molding, in: Proceedings of the IEEE International Workshop on Micro Electro Mechanical System (MEMS'93), 1993, pp. 42–47.
[3] S. Maruo, K. Ikuta, Submicron stereolithography for the production of freely movable mechanisms by using single-photon polymerisation, Sens. Actuators A 100 (2002) 70–76.
[4] S. Kawata, H.-B. Sun, T. Tanaka, K. Takada, Nature 412 (2001) 697.
[5] X.N. JIang, C. Sun, X. Zhang, B. Xu, Y.H. Ye, Microstereolithograhy of lead zirconate titanate thick film on silicon substrate, Sens. Actuators A 87 (2000) 72–77.
[6] C.H. Mastrangelo, C.H. Hsu, Mechanical stability and adhesion of microstructures under capillary forces. Part I. Basic theory, J. Microelectromech. Syst. 2 (1993) 33–43.
[7] C.H. Mastrangelo, C.H. Hsu, Mechanical stability and adhesion of microstructures under capillary forces. Part II. Experiments, J. Microelectromech. Syst. 2 (1993) 44–55.
[8] C.-J. Kim, J.Y. Kim, B. Sridharan, Comparative evaluation of drying techniques for surface micromaching, Sens. Actuators A 64 (1998) 17–26.
[9] G.T. Mulhern, D.S. Soane, R.T. Howe, Supercritical carbon dioxide drying of microstructurs, in: Proceedings of the Seventh International Conference on Solid-State Sensors and Actuators (Transducers'93), Yokohama, Japan, June 7–10, 1993, pp. 296–299.
[10] H. Guckel, J.J. Sniegowski, T.R. Christenson, Advances in processing techniques for silicon micromechanical devices with smooth surfaces, in: IEEE Micro Electro Mechanical Systems Workshop, Salt Lake City, UT, USA, 1989, pp. 71–75.
[11] K. Deng, R.J. Collins, M. Mehregany, C.N. Sukkenik, Performance impact of monlayer coating of polysilicon micromotors, in: IEEE Micro Electro Mechanical Systems Workshop, Amsterdam, The Netherlands, 1995, pp. 368–373.
[12] D. Wu, N. Fang, C. Sun, X. Zang, Adhesion force of polymeric three-dimensional microstructures fabricated by microstereolithography, Appl. Phys. Lett. 81 (2002) 3963–3965.
[13] P.F. Jacobs, Rapid Prototyping & Manufacturing, Society of Manufacturing Engineering, Dearborn, 1992, pp. 221–245 (Chapter 9).
[14] C. Sun, N. Fang, X. Zhang, Proceeding of the 2001 ASME International Mechanical Engineering Congress and Exposition, MEMS, vol. 3, New York, NY, 2001, pp. 813–818.
[15] E. Manias, J. Chen, N. Fang, X. Zhang, Appl. Phys. Lett. 79 (2001) 1700–1702.

Biographies

Dongmin Wu received his PhD in Mechanical Engineering from University of California at Los Angeles in 2005. He is currently a postdoc researcher in Mechanical Engineering Department, UC Berkeley. His research interests are in 3D micro-fabrication, plasmonic optics and molecular electronics.

Nicholas Fang received his PhD in Mechanical Engineering from University of California Los Angeles in 2004. He is currently an assistant professor in Department of Mechanical and Industrial Engineering, University of Illinois Urbana-Champaign. His research interest includes the 3D micro and nanolithography, design and manufacturing photonic metamaterials and devices, energy transfer and mass transport phenomena in micro/nano/biosystems.

Cheng Sun received his PhD in Industrial Engineering from Pennsylvania State University in 2002. He is currently the Chief Operating Officer at the Center for Scalable and Integrated Nanomanufacturing at University of California Los Angeles. His research interest includes the novel 3D micro- and nano-fabrication technologies and the device applications.

Xiang Zhang received his PhD from UC Berkeley (1996). He was an assistant professor at Pennsylvania State University (1996–1999), and associate professor (1999–2003) and full professor (2003–2004) at UCLA. He joined UC Berkeley faculty in July 2004. Currently, he serves as the Chancellor's Professor and the Director of NSF Nano-scale Science and Engineering Center. His research interests include Micro-nano scale engineering, novel 3D fabrication technologies in microelectronics and photonics, micro and nano-devices, nano-lithography and nano-instrumentation, rapid prototyping, bio-MEMS, and semiconductor manufacturing.